



Electronically Controlled Shock Absorber System Used as a Road Sensor Which Utilizes Super Sonic Waves

Author(s): Fukashi Sugasawa, Hiroshi Kobayashi, Toshihiko Kakimoto, Yasuhiro Shiraishi and Yoshiaki Tateishi

Source: *SAE Transactions*, Vol. 94, Section 6 (1985), pp. 15-25

Published by: SAE International

Stable URL: <https://www.jstor.org/stable/44742911>

Accessed: 19-07-2020 19:55 UTC

JSTOR is a not-for-profit service that helps scholars, researchers, and students discover, use, and build upon a wide range of content in a trusted digital archive. We use information technology and tools to increase productivity and facilitate new forms of scholarship. For more information about JSTOR, please contact support@jstor.org.

Your use of the JSTOR archive indicates your acceptance of the Terms & Conditions of Use, available at <https://about.jstor.org/terms>



JSTOR

SAE International is collaborating with JSTOR to digitize, preserve and extend access to *SAE Transactions*

Electronically Controlled Shock Absorber System Used as a Road Sensor Which Utilizes Super Sonic Waves

Fukashi Sugasawa,
Hiroshi Kobayashi,
Toshihiko Kakimoto,
Yasuhiro Shiraishi,
and Yoshiaki Tateishi

Nissan Motor Co., Ltd.

ABSTRACT

An important factor in the development of vehicle suspensions has been how to get higher performance from both ride and stability, which are normally in conflict. In addressing this problem, we analyzed the optimum damping forces of shock absorbers for various driving conditions and developed an electronically controlled shock absorber system, which we call "Super Sonic Suspension" based on the results.

Through this microcomputer-controlled system, we achieved a great improvement in riding comfort by being able to the damping force much lower than before, based on the results of said analysis.

At the same time, stability of the vehicle was also improved by optimumly controlling the damping force for various driving conditions through signals from a newly developed road sensor, which utilizes supersonic waves, and other sensors.

1. INTRODUCTION

A traditional issue in automobile suspension design has been the question of how to satisfy at the highest level possible the contradictory requirements for ride and stability.

As one result of the rapid advances made in electronic control technology, control systems are now being applied to the automobile which resolve this problem by varying the damping force of the shock absorbers according to the running conditions. A key factor in such systems is the control software, the development of which includes the task of determining the control values and conditions for controlling the damping force.

In this investigation, the optimum damping force for various running conditions was first found through linear analyses. The results obtained were then utilized to develop a system that provides maximum control effectiveness.

Ride quality has been improved with this system by setting the damping force, which serves as the basic parameter, at a lower level than ever before. The system also employs a newly developed road sensor that can easily detect light, bouncy vibrations induced by inputs from the road surface. Hitherto the detection of such vibrations has been exceedingly difficult.

Owing to these improvements, this system displays maximum control effectiveness and provides damping force control that matches human sensation.

2. DAMPING FORCE OPTIMIZATION

The relationship between damping force and vehicle behavior was clarified through linear analyses. Optimum damping forces were then set for various running conditions in order to improve ride and road holding performance and reduce roll, pitch and bouncing.

2.1 IMPROVEMENT OF RIDE AND ROAD HOLDING PERFORMANCE - Basic Eqs. (1) and (2) are derived from the model illustrated in Fig. 1 which has two degrees of freedom.

$$m_1 \ddot{x}_1 + c_2 (\dot{x}_1 - \dot{x}_2) + k_1 (x_1 - x_0) + k_2 (x_1 - x_2) = 0 \quad (1)$$

$$m_2 \ddot{x}_2 + c_2 (\dot{x}_2 - \dot{x}_1) + k_2 (x_2 - x_1) = 0 \quad (2)$$

m_1, m_2 : masses
 c_2 : damping constant
 k_1, k_2 : spring constants
 x_0, x_1, x_2 : displacements
0 : road surface
1 : unsprung
2 : sprung

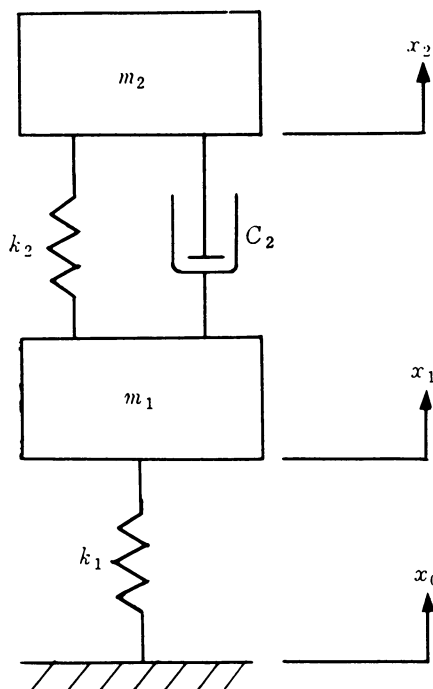


Fig. 1 Analytical model for ride

A Laplace transformation is performed on these equations and the transfer functions of the sprung acceleration \ddot{X}_2 and the unsprung relative displacement $X_1 - X_0$ in relation to the road surface displacement X_0 are found. These operations yield Eqs. (3) and (4).

$$H_1(s) = \frac{S^2 \cdot X_2(s)}{X_0(s)} = \frac{2\zeta\omega_1^2\omega_2 \cdot S^3 + \omega_1^2\omega_2^2 S^2}{S^4 + 2\mu\zeta\omega_2 \cdot S^3 + (\omega_1^2 + \mu\omega_2^2) \cdot S^2 + 2\zeta\omega_1^2\omega_2 \cdot S + \omega_1^2\omega_2^2} \quad (3)$$

$$H_2(s) = \frac{X_0(s) - X_1(s)}{X_0(s)} = \frac{S^4 + 2\mu\zeta\omega_2 \cdot S^3 + \mu\omega_2^2 \cdot S^2}{S^4 + 2\mu\zeta\omega_2 \cdot S^3 + (\omega_1^2 + \mu\omega_2^2) \cdot S^2 + 2\zeta\omega_1^2\omega_2 \cdot S + \omega_1^2\omega_2^2} \quad (4)$$

$$\omega_1^2 = k_1/m_1, \quad \omega_2^2 = k_2/m_2, \\ \mu = (m_1 + m_2)/m_1, \quad \zeta = c_2/2\sqrt{m_2 k_2}$$

The overall power P of the vehicle's vertical acceleration and the load fluctuation rate R are used as the evaluation criterion for ride and road holding performance, respectively. First, we shall find the overall power P .

From Eq. (3) the vehicle's vertical acceleration $G(s)$ is expressed as:

$$G(s) = S^2 \cdot X_2(s) = S^2 \cdot H_1(s) \cdot X_0(s)$$

Hence, assuming $X_0(s)$ is given by the relationship

$$X_0(s) = A/s \quad (5)$$

which is an abbreviated equation of the ISO standard and A is a constant, we obtain

$$G(s) = A \cdot S \cdot H_1(s) \quad (6)$$

Since the overall power P is defined as

$$P = \int_0^\infty (G(s))^2 d\omega$$

by substituting Eq. (6) into this definition and transforming ω into S , we obtain.

Substituting Eq. (3) into this expression and solving for P yields the following equation:

$$P = \pi A^2 \frac{4\zeta^2\omega_1^2\omega_2 + \mu\omega_2^3}{4(\mu-1)\zeta} \quad (7)$$

Next, we shall find the load fluctuation rate R .

The rate of change R is defined as

$$R = \frac{k_1}{(m_1 + m_2)g} \cdot \bar{\sigma}$$

where $\bar{\sigma}$ is the root-mean-square value of $X_0 - X_1$ and g is the acceleration of gravity. Then, in the same manner as for the overall power, the following equation is found from Eqs. (4) and (5):

$$R = \sqrt{\frac{\pi A \omega_1^4 (4\beta\mu^2\zeta^2 + \beta^2\mu^3 - 2\beta\mu + 1)}{4g^2\mu(\mu-1)\zeta\omega_2}} \quad (8)$$

$$\left(\beta = \frac{\omega_2^2}{\omega_1^2}\right)$$

Viewing Eqs. (7) and (8) as functions of ζ , it is seen that each of them has a minimum value. The value of ζ at that time we shall let represent the optimum damping ratio ζ_{op} . Then, ζ_{op} can be expressed with the following equations, respectively:

$$\text{Ride } \zeta_{op} = \frac{1}{2} \sqrt{\frac{\mu \cdot \alpha}{\mu - 1}} \quad (9)$$

Road holding performance

$$\zeta_{op} = \frac{1}{2} \sqrt{\frac{\mu^3 \alpha^2 - 2\mu(\mu-1)\alpha + (\mu-1)^2}{\mu^2(\mu-1)\alpha}} \quad (10)$$

The optimum damping ratio ζ_{op} is different for ride and road holding performance. The relationship between the minimum value of each evaluation criterion and the damping ratio ζ is shown in Fig. 2 for a compact passenger car. In this figure the evaluation criterion have been translated into non-dimensional values.

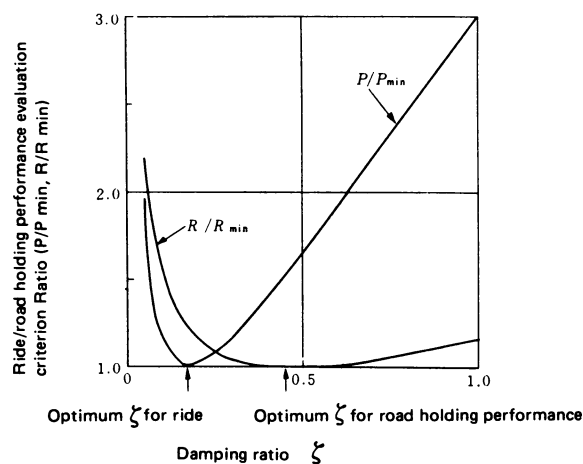


Fig. 2 The relationship between the damping ratio and ride and road holding performance (for a compact passenger car)

2.2 ROLL AND PITCH REDUCTION - Equation (11) is derived as a basic equation of turning motion from the model illustrated in Fig. 3. In addition, Eq.(12) is also derived from this model as the transfer function of the turning angle θ in relation to the moment M .

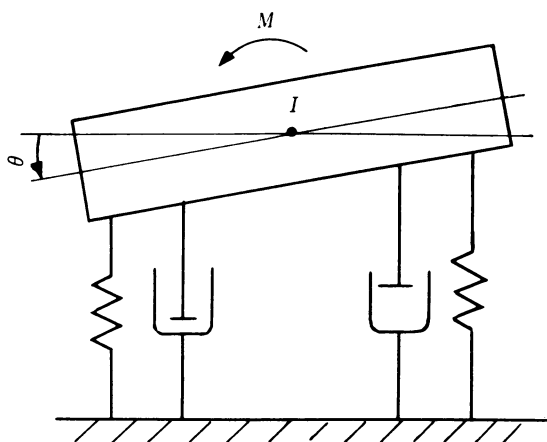


Fig. 3 Analytical model for roll and pitch

$$M = I\ddot{\theta} + c\dot{\theta} + K\theta \quad (11)$$

$$H(S) = \frac{\theta(S)}{M(S)} = \frac{1}{I} \cdot \frac{1}{S^2 + 2\zeta\omega_0 S + \omega_0^2} \quad (12)$$

$$\zeta = C/(2\sqrt{I \cdot K}), \quad \omega_0^2 = K/I$$

M : moment
 I : moment of inertia
 θ : turning angle
 C : turning damping constant
 K : turning spring constant

The gain characteristics of Eq.(12) are shown in Fig. 4. In terms of the best damping effect, the condition that keeps the maximum gain below the normal gain is $\zeta \geq 1/\sqrt{2}$. However, when ride is considered and the minimum value is adopted, the optimum damping ratio becomes $\zeta_{op} = 1/\sqrt{2}$.

Hence, the following equations are obtained from the damping ratios for roll and pitch:

$$\text{Roll } \zeta_{op} = \frac{T_F^2 \cdot C_F + T_R^2 \cdot C_R}{4\sqrt{I_R} \cdot (K_F + K_R)} = \frac{1}{\sqrt{2}} \quad (13)$$

$$\text{Pitch } \zeta_{op} = \frac{L_F^2 \cdot C_F + L_R^2 \cdot C_R}{\sqrt{2} \cdot I_P (L_F^2 \cdot k_F + L_R^2 \cdot k_R)} = \frac{1}{\sqrt{2}} \quad (14)$$

I_R, I_P : Roll and pitch moments of inertia
 K_F, K_R : Front and rear roll stiffnesses
 k_F, k_R : Front and rear spring constants
 C_F, C_R : Front and rear damping constants
 T_F, T_R : Front and rear treads
 L_F, L_R : Distances between front and rear tires and pitch center

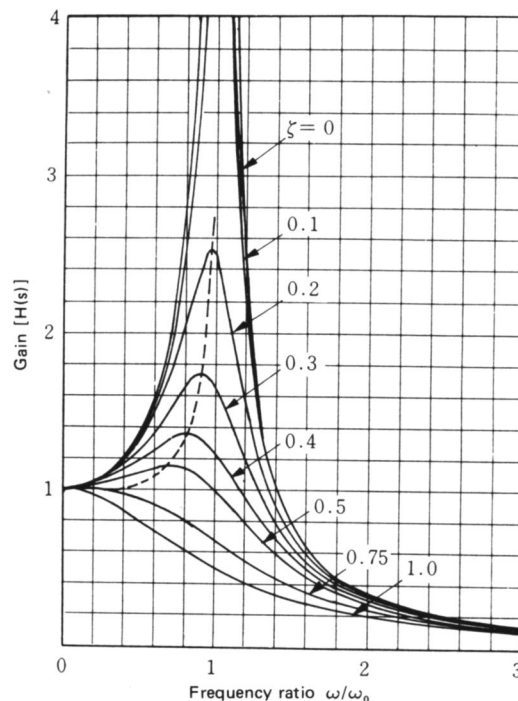


Fig. 4 Gain characteristics of roll and pitch

2.3 BOUNCING REDUCTION - Equation (15) is derived as a basic equation of the vehicle's vertical motion from the model illustrated in Fig. 5. Also obtained is Eq.(16) for the transfer function of the vehicle displacement X_2 in relation to the road surface displacement X_0 .

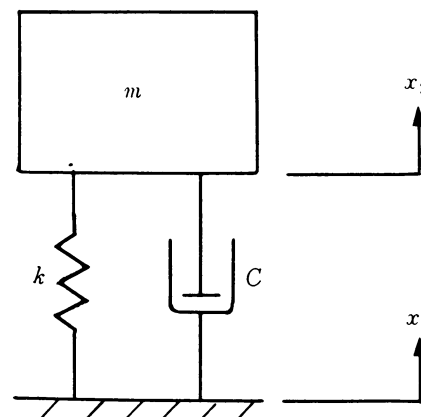


Fig. 5 Analytical model for bouncing

$$m\ddot{x}_2 + c(\dot{x}_2 - \dot{x}_0) + k(x_2 - x_0) = 0 \quad (15)$$

$$H(S) = \frac{x_2(S)}{x_0(S)} = \omega_0^2 \frac{1 + (2\zeta/\omega_0)S}{S^2 + 2\zeta\omega_0 S + \omega_0^2} \quad (16)$$

$$\zeta = c/(2\sqrt{mk}), \quad \omega_0^2 = k/m$$

The gain characteristics of Eq.(16) are given in Fig. 6. It is seen that a satisfactory damping effect is obtained provided that the damping ratio ζ is $1/\sqrt{2}$, which is the same value as for roll.

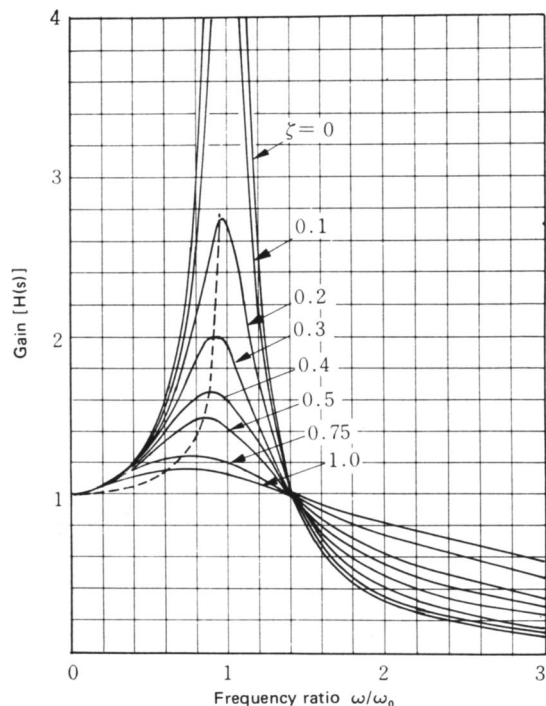


Fig. 6 Gain characteristics of bouncing

However, unlike roll, bouncing usually occurs when travelling on a heaving road. Consequently, in order to give due consideration to ride, an intermediate value between $1/\sqrt{2}$ and the value obtained from Eq.(9) is selected as the optimum damping value for bouncing. This yields the following equation:

$$\text{Bouncing } \zeta_{op} = \frac{\sqrt{2}}{4} + \frac{1}{4} \sqrt{\frac{\mu\alpha}{\mu-1}} \quad (17)$$

The foregoing results have been summarized in Table 1 as the optimum damping ratios for various running conditions.

Table 1 Optimum Damping Ratios for Various Running Conditions

RUNNING CONDITION	CONTROL OBJECTIVE	OPTIMUM CONDITION	OPTIMUM DAMPING RATIO	
			THEORETICAL VALUE	FOR COMPACT CAR
ORDINARY DRIVING	RIDE IMPROVEMENT	TO MINIMIZE SPRUNG OVERALL ACCELERATION	$\zeta \left(= \frac{c_2}{2\sqrt{m_2 k_2}} \right) = \frac{1}{2} \sqrt{\frac{\mu\alpha}{\mu-1}}$	0.16
ROLL	ROLL REDUCTION WHEN TURNING	TO SUPPRESS DYNAMIC ROLL ANGLE TO A LEVEL BELOW STATIC ROLL ANGLE	$\zeta \left(= \frac{T_F^2 \cdot C_F + T_R^2 \cdot C_R}{4\sqrt{I_R (K_F + K_R)}} \right) = \frac{\sqrt{2}}{2}$	0.71
PITCH	PITCH REDUCTION WHEN ACCELERATING, DECELERATING AND BRAKING	TO SUPPRESS DYNAMIC PITCH ANGLE TO A LEVEL BELOW STATIC PITCH ANGLE	$\zeta \left(= \frac{L_F^2 \cdot C_F + L_R^2 \cdot C_R}{\sqrt{2I_p (L_F^2 \cdot k_F + L_R^2 \cdot k_R)}} \right) = \frac{\sqrt{2}}{2}$	0.71
BOUNCING	REDUCTION OF BOUNCY FEELING AND RIDE IMPROVEMENT	TO SUPPRESS LIGHT, BOUNCY VIBRATIONS WITHIN A RANGE WHERE RIDE QUALITY DOESN'T DETERIORATE	$\zeta \left(= \frac{c_2}{2\sqrt{m_2 k_2}} \right) = \frac{\sqrt{2}}{4} + \frac{1}{4} \sqrt{\frac{\mu\alpha}{\mu-1}}$	0.43
ROUGH ROAD	ROAD HOLDABILITY IMPROVEMENT	TO MINIMIZE THE ROOT-MEAN-SQUARE VALUE OF UNSPRUNG RELATIVE DISPLACEMENT	$\zeta \left(= \frac{c_2}{2\sqrt{m_2 k_2}} \right) = \frac{1}{2} \sqrt{\frac{\mu^3 \alpha^2 - 2\mu(\mu-1)\alpha + (\mu-1)^2}{\mu^2(\mu-1)\alpha}}$	0.44

m : MASS
 I : MOMENT OF INERTIA
 k : SPRING CONSTANT
 K : ROLL STIFFNESS

C : DAMPING CONSTANT
 ζ : DAMPING RATIO
 T : TREAD
 L : DISTANCE BETWEEN TIRES AND PITCH CENTER

(1: UNSPRUNG
 2: SPRUNG
 F: SPRUNG FRONT
 R: SPRUNG REAR)

$\alpha = \frac{k_2}{k_1}$
 $\mu = \frac{m_1 + m_2}{m_1}$

3. CONTROL SPECIFICATIONS

The new system allows three-level control over the damping force based on the analytical results explained in the previous section. With the soft setting, the power spectrum of the vehicle's vertical acceleration is minimized for ordinary running conditions. The medium and hard settings provide optimum values for road holding performance and bouncing and roll and pitch, respectively. The three levels and the relevant equations are summarized below.

Soft ----- ride comfort Eq. 6

Medium ----- road holding performance and bouncing Eqs. 7 and 14

Hard ----- roll and pitch Eqs. 10 and 11

The occurrence of roll and pitch can be predicted from various driving operations such as steering, accelerating, decelerating and braking. Consequently, it is relatively easy to suppress roll and pitch by raising the damping force in advance. However, the light bouncy vibrations induced by irregularities and undulations in the road surface have traditionally been very difficult to detect and to control accurately in accordance with human sensation. One reason for this is that the generating cause is not on the vehicle side; another reason is that such vibrations give vehicle occupants a feeling of discomfort that is disproportionate to the small vibration level. The detection and control difficulties have thus been obstacles to the lowering of the ordinary damping force.

The newly-developed road sensor incorporated in this control system utilizes supersonic pulses to measure the vehicle height from the road. Judgments as to the road condition, such as rough road or heaving road, are made from the pattern of fluctuation in vehicle height. Based on such judgments the system executes fine control that matches human sensation and thereby achieves maximum control effectiveness.

The following gives a concise explanation of each control item.

3.1 ROLL CONTROL - The occurrence of roll is suppressed by detecting quick steering operation with a steering angle sensor. Detection sensitivity is raised in proportion to vehicle speed.

3.2 PITCH CONTROL - Nose-diving and shaking during hard braking are suppressed by estimating the deceleration speed from the change speed in vehicle height, i.e. amount of diving. In addition, the increase or decrease in engine torque is judged from the change in the ECCS fuel injection pulse width, and this information is used for pitch control during acceleration and deceleration. (ECCS: Electronic Concentrated engine Control System)

3.3 BOUNCING CONTROL - Single bumps or dips are detected from large changes in vehicle height and this information is utilized to prevent the subsequent occurrence of light, bouncy vibrations. Moreover, light, bouncy vibrations that occur when travelling on a heaving road are detected from cyclic changes in vehicle height and effectively suppressed.

It is generally true that steady vibrations tend to decrease with increasing vehicle speed and, as a result even, small vibrations become a source of discomfort at high speed. Therefore, in this system the detection sensitivity of these controls is increased in proportion to vehicle speed.

3.4 ROAD HOLDING PERFORMANCE CONTROL - Based on the pattern of fluctuation in vehicle height, the system judges that the vehicle is running on a rough road and makes adjustments to assure good road holding performance.

3.5 HIGH-SPEED STABILITY CONTROL - To improve high-speed stability, the damping force at the front is raised and the understeer tendency of the vehicle is strengthened.

3.6 CONTROL DURING STOPPING - Damping force is increased during stopping to suppress shaking as well as to suppress rocking when passengers

enter or exit the vehicle.

A summary of the control objectives, detection conditions and sensors is given in Table 2.

Table 2 Summary of Damping Force Control System

CONTROL OBJECTIVES		DETECTION CONDITIONS	SENSORS USED					DAMPING FORCE (FRONT REAR)
			VEHICLE SPEED	STEERING ANGLE	ACCEL/ DECEL	BRAKE	ROAD CONDITION	
ROLL	ROLL REDUCTION FOR QUICK STEERING OPERATION	WHEN STEERING OPERATIONS ARE MADE FASTER THAN PREDETERMINED STEERING SPEED	○	○				H H
PITCH	REDUCTION OF NOSE-DIVING AND SHAKING INDUCED BY BRAKING	WHEN NOSE-DIVING DUE TO BRAKING IS GREATER THAN PREDETERMINED VALUE				○	○	H H
	REDUCTION OF PITCHING WHEN ACCELERATING AND DECELERATING	WHEN CHANGE IN ENGINE TORQUE IS GREATER THAN PREDETERMINED VALUE	○		○			M M
BOUNCING	REDUCTION OF LIGHT, BOUNCY VIBRATIONS IN BOTTOMING WHEN VEHICLE HITS SINGLE BUMP	WHEN LARGE FLUCTUATION OCCURS IN VEHICLE HEIGHT	○				○	M M
	REDUCTION OF LIGHT, BOUNCY VIBRATIONS IN BOUNCING ON A HEAVING ROAD	WHEN CYCLE FLUCTUATION OCCURS IN VEHICLE HEIGHT	○				○	M M
ROAD HOLDING PERFORMANCE	ROAD HOLDING PERFORMANCE IMPROVEMENT WHEN RUNNING ON ROUGH ROADS	WHEN VEHICLE HEIGHT FLUCTUATION INDICATES ROUGH ROAD RUNNING PATTERN	○				○	M M
OTHERS	STABILITY IMPROVEMENT AT HIGH SPEEDS	WHEN VEHICLE SPEED IS ABOVE PREDETERMINED VALUE	○					M S
	PREVENTION OF SHAKING WHEN STOPPING AND ROCKING WHEN PASSENGERS EXIT OR ENTER	WHEN VEHICLE SPEED IS BELOW PREDETERMINED VALUE	○					H H

H: HARD M: MEDIUM S: SOFT

4. CONTROL SYSTEM

4.1 SYSTEM STRUCTURE - The structure of the control system is illustrated in Fig. 7. A total of five sensors including the newly developed supersonic road sensor are employed to detect the running conditions. The sensor signals are fed into the microcomputer of the control unit which determines the optimum damping force according to the running conditions. Control signals are then sent to adjust the damping force of variable shock absorbers to the optimum values.

One of the prominent advantages of this system is that through the use of the road sensor it can provide optimum control in accordance with the actual road conditions.

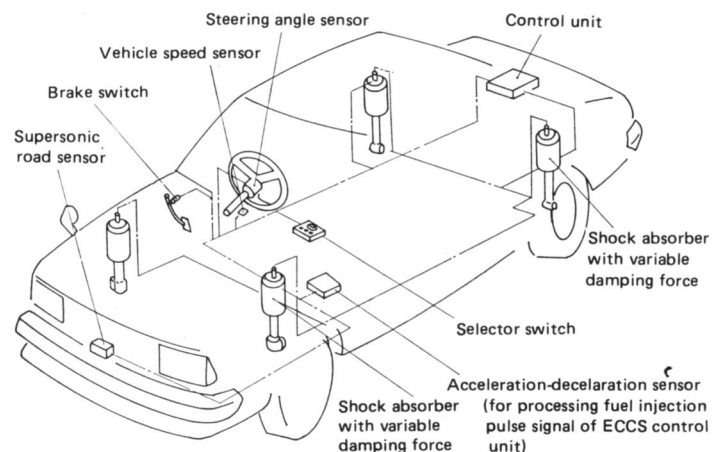


Fig. 7 Schematic diagram of system structure

4.2 SHOCK ABSORBERS WITH VARIABLE DAMPING FORCE - The structure of the shock absorber is illustrated in Fig. 8.

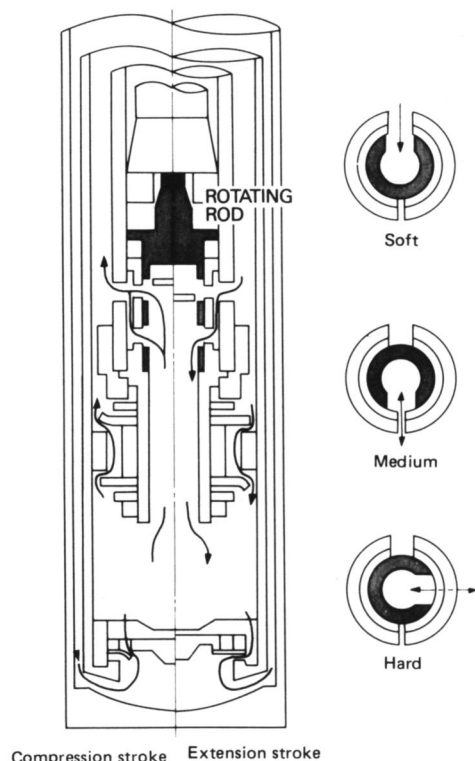


Fig. 8 Structure of shock absorber

A built-in motor turns a rotary valve to select the orifice diameter for three different damping levels: soft, medium and hard. This three-level design makes it possible to provide both a softer and a more stable driving feeling.

The stopping position of the rotary valve is accurately controlled with an encoder signals. The damping force is switched from one damping level to another rapidly enough to ensure that the full control effect is obtained.

4.3 SUPERSONIC ROAD SENSOR - As illustrated in Fig. 9, the vehicle height is calculated on the basis of the reflection time T it takes an supersonic waves to propagate to the ground and return again to the receiver. Judgment of the road condition is made by analyzing the pattern of change in the vehicle height.

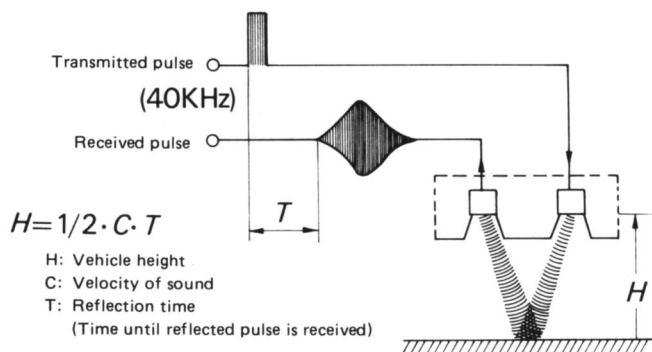


Fig. 9 Principle of vehicle height measurement

Distinctive features of this sensor include two important improvements that were made to a conventional supersonic distance sensor. The first is that it can measure short distances accurately, something that conventional sensors cannot do. The second is that it provides accurate measurements irrespective of the road surface.

o. Sensor Structure - A schematic diagram showing the structure of the supersonic sensor is given in Fig. 10. The transmitter and receiver are covered with an insulator and their apertures are shaped like an acoustic horn in order to improve the directivity pattern. The associated amplifier and signal processing circuitry are also housed in the sensor case.

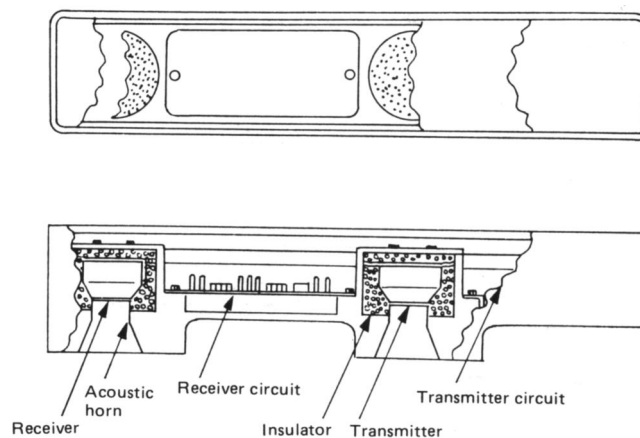


Fig. 10 Sensor structure

o. Improvement of Measuring Short Distances Accurately - In the measurement of short distances, it is difficult to discriminate between the direct waves from the transmitter and the reflected waves from the road surface because the difference of the arrival times is very small. If the distance is calculated by the direct waves instead of the reflected waves it shortens the reflection time T . Then it is important to separate the direct waves from the reflected waves for accurate measurement. The supersonic road sensor has three improvements. The first is selection of insulating material. This decreases the direct waves conducted through the insulator. Since rubber is harder in low temperature, the direct waves increase in response to the temperature drop. But we can reduce the direct waves by using insulating rubber which is soft even in low temperatures. The second is optimizing the shape of acoustic horns. This decreases the direct waves propagated through air. The directivity of the transmitter and receiver is influenced by the shape of acoustic horns.

The directivity is shown in Fig. 11.

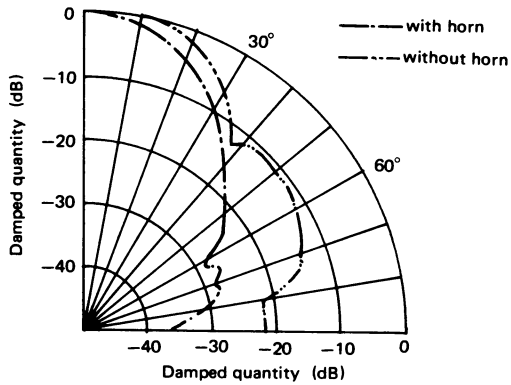


Fig. 11 Improvement of directivity

The side lobe is decreased by the acoustic horn. The third is improving the sensor circuit. This separates the direct wave signal from the reflected wave signal by adopting an electronically produced circumvention signal. This is shown in Fig. 12. By these improvements we can separate the direct waves from the reflected waves and obtain an accurate measurement.

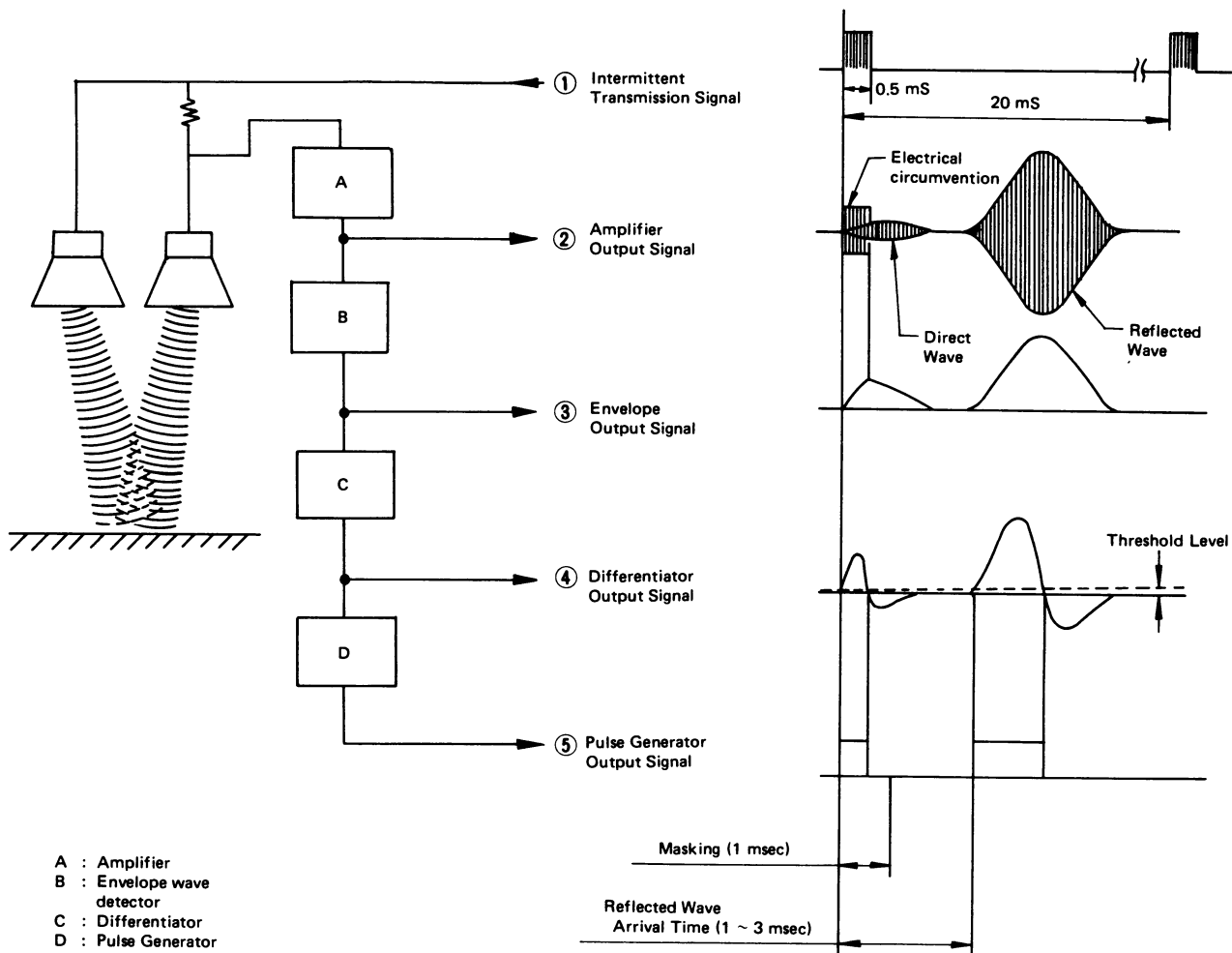


Fig. 12 Block diagram and wave forms of electrical processing method

。 Signal Processing Method - The signal processing method used to calculate the vehicle height is illustrated in Fig. 13. The vehicle height is initially calculated from the reflection time. Compensation is then added according

to the intensity of the reflected waves and judgement is made as to the validity of the height value. Any data judged abnormal are excluded and then the signal is filtered to obtain the vehicle height.

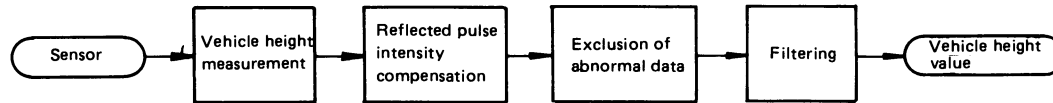


Fig. 13 Block diagram of vehicle height signal processing method

Reflected waves intensity compensation is performed to avoid erroneously higher judgements of the vehicle height, which the processing circuitry would otherwise make due to the delayed reception of weak reflected waves.

Different types of noise also occur in the vehicle height measurement utilized supersonic waves. Completely random noise can be caused by external disturbance and high-frequency noise can be induced by components that the reflected wave intensity compensation cannot fully correct as well as by other causes. The former noise is removed in the process of excluding abnormal data and the latter noise is removed by filtering, in order to obtain an accurate vehicle height value.

The measurement characteristics of the vehicle height obtained in this fashion are shown in Fig. 14. At a distance of 15 cm or more, measurements can be made to within a resolution of 2 mm at room temperature.

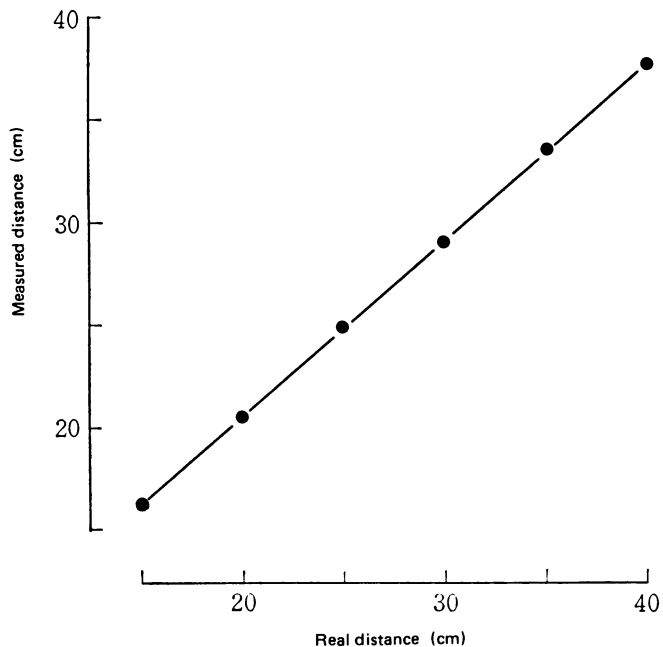


Fig. 14 Measurement characteristics

Furthermore, measurement accuracy is not affected by diffused reflection caused by the form of the road surface (i.e. gravel, etc.) or by the difference of the reflection rate due to the presence of sand, snow or other matter on the road.

Accurate measurement is obtained for a variety of surfaces ranging from asphalt to gravel and snow-covered roads.

。 Road Condition Judgment - The conditions determining whether the damping force should be increased are different for ride improvement and road holding performance improvement. Consequently, in judging the road condition from fluctuations in vehicle height, a distinction must first be made between a heaving road and a rough road. Then, based on separate judgment criteria for each type, a decision must be made as to whether the damping force should be increased or not.

The results of the frequency analysis of vehicle height fluctuations for three typical road conditions are presented in Fig. 15. As the results indicate, the frequency components of a heaving road and of a rough road are different

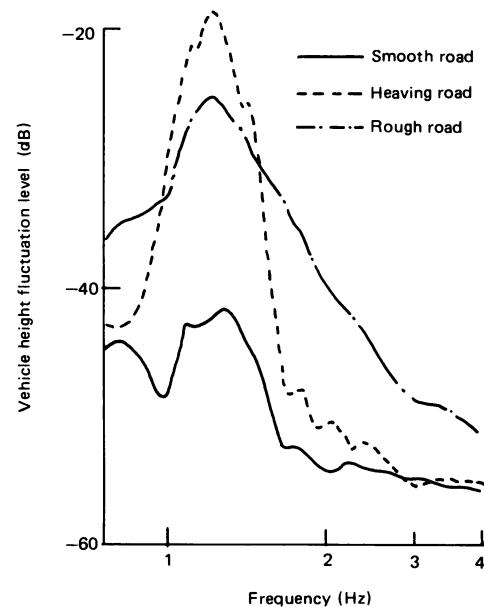


Fig. 15 Frequency analysis of vehicle height

above approximately 2 Hz. Therefore, this difference can be used to distinguish between these two types of roads. In this detection approach, the high-frequency components above approximately 2 Hz was detected separately from the low-frequency components below this level, which consist mainly of components near the sprung resonance frequency. Then, based on the magnitude of the

high-frequency components, judgment is made as to whether the road is heaving or rough. A separate standard is provided for judging the low-frequency components, and based on this standard a decision is made as to whether the damping force should be raised or not.

An outline of the road surface judgment logic is given in Table 3.

Table 3 Road Condition Judgment Logic

	LOW-FREQUENCY COMPONENTS		
		SMALL	LARGE
HIGH-FREQUENCY COMPONENTS			
SMALL		SMOOTH ROAD (DAMPING FORCE CONTROL UNNECESSARY)	HEAVING ROAD
LARGE			ROUGH ROAD

5. CONTROL RESULTS

5.1 RIDE IMPROVEMENT EFFECT - The overall power of the floor vertical acceleration when travelling on a rough road is shown in Fig. 16 as a non-dimensional value at the optimum damping ratio. In comparison with a typical car (equivalent to the medium setting), the soft setting in this system reduces the overall power about 13%.

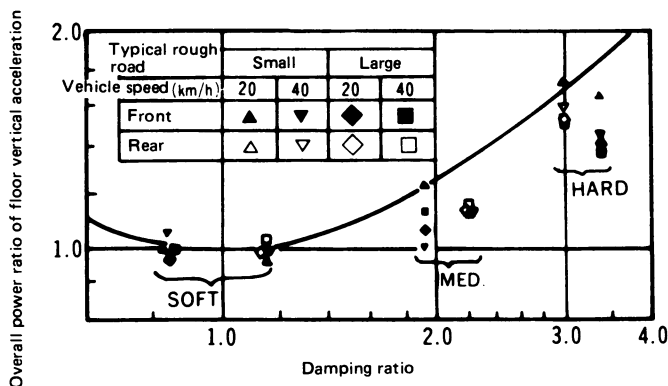


Fig. 16 Damping ratio and floor vertical acceleration

5.2 VIBRATION SUPPRESSION EFFECT - The reduction achieved in the roll angle (difference in left-right wheel travel) when making quick steering operation is shown in Fig. 17. The change in the roll angle is suppressed by predicting the lateral acceleration (G) from the vehicle speed and steering speed and increasing the damping force accordingly.

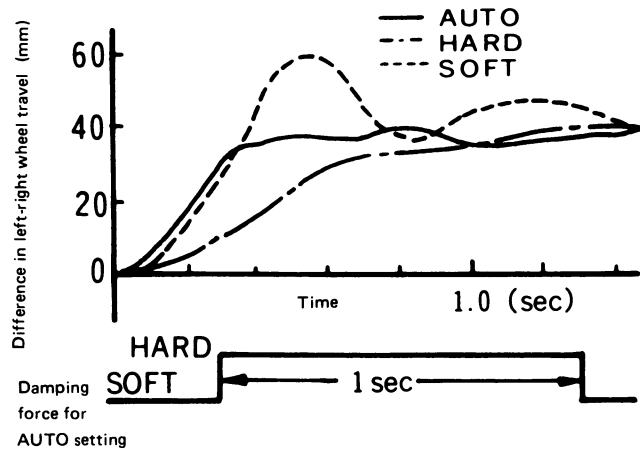


Fig. 17 Roll angle for step-steer (steering angle: 30 degree; vehicle speed: 60 km/h)

The reduction achieved in the pitch angle (difference in front-rear wheel travel) when braking and stopping is shown in Fig. 18. Nose-diving is suppressed by judging the deceleration speed from the change speed in vehicle height when the braking signal is received and switching the damping force to the optimum level. At the same time, front-end shaking is similarly suppressed by detecting stopping from the vehicle speed signal.

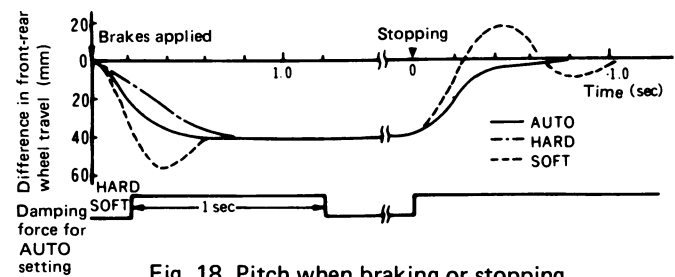


Fig. 18 Pitch when braking or stopping

By predicting the occurrence of roll and pitch from the sensor signals and controlling the damping force to the optimum level, there is no overshooting and the vehicle inclination is kept to a minimum.

The reduction achieved in bouncing on a heaving road is shown in Fig. 19. In this case, large body vibrations are detected and the subsequent occurrence of light, bouncy vibrations is suppressed by increasing the damping force.

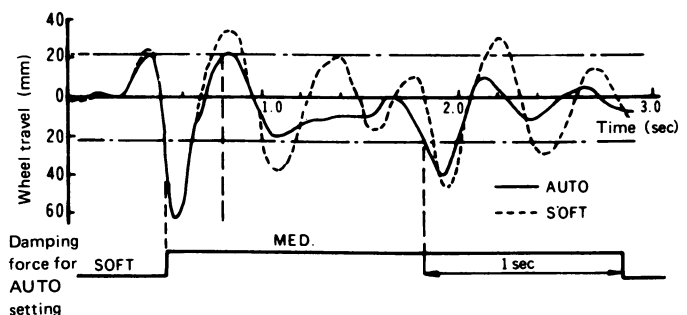


Fig. 19 Body vibration on a heaving road

6. CONCLUSION

In this investigation the optimum damping ratios for typical running conditions were found through linear analyses. Based on the results obtained, a control system has been designed with three levels of damping force which are automatically selected to provide optimum ride and stability.

For ordinary driving the soft damping force setting is selected to improve ride quality. The damping force is raised to the medium or hard setting, depending on the running conditions, so as to suppress changes in the vehicle posture. In order to set the damping force of the soft setting at a lower level than ever before, special measures had to be taken to suppress the light, bouncy vibrations induced by irregularities in the road surface.

The key element of those measures is a newly developed road sensor which allows accurate detection of road conditions. As a result, the control system provides optimum control performance that matches human sensation.